A SENSOR ARM FOR ROBOTIC ANTARCTIC METEORITE SEARCH

Chris Urmson, Ben Shamah, James P. Teza, Michael D. Wagner, Dimitrios Apostolopoulos, William "Red" Whittaker

Field Robotics Center, The Robotics Institute, Carnegie Mellon University, Pittsburgh PA 15213

Phone: (412) 268-8098; Fax: (412) 268-5895

e-mail: {curmson, bshamah, jpt, mwagner, da1v, red}@ri.cmu.edu

Abstract: In January 2000 the Nomad robot searched an area of blue ice in Antarctica and autonomously classified 5 in-situ meteorites. The robotic capabilities of search and target identification, coupled with the scientific capabilities of analysis and classification of rocks in an extreme environment were made possible by the integration of many different technologies for both hardware and software. This paper focuses on the development and integration of the sensor arm used to deploy a spectrometer from a multi-meter scale robot to centimeter scale rocks. The sensor arm combines off the shelf hardware for motion control, actuation, and sensing. Available techniques were applied in the areas of kinematics, visual servoing and image segmentation. The successful demonstration of the robotic search for Antarctic meteorites serves as a benchmark for the advancement of both custom designed and off the shelf robotic technologies.

Keywords: meteorite search, visual servoing, robotic sensor placement, robot arm

1. INTRODUCTION

For decades, geologists have searched Antarctica's moraines for meteorites. While successful, these searches have been expensive and difficult due to the harsh Antarctic conditions. An automated meteorite search using a robotic platform could minimize the hazards and costs inherent to these expeditions, and provide a tireless and thorough search assistant to human teams exploring extreme locales on Earth. Robotic Antarctic meteorite search is also an analog for geologic missions to other planets.

Nomad is a semi-autonomous rover capable of exploring rugged terrain. Nomad was originally developed to demonstrate and evaluate technologies that could be applied to long duration planetary exploration. In 1997 Nomad traversed 220 km in the Atacama desert of southern Chile [Bapna et al, 1998].

In 1998 the Robotic Antarctic Meteorite Search program was chartered to develop a robot capable of searching Antarctic terrain for meteorites. To accomplish this goal the problem of meteorite search was broken down into search, detection, classification, and locomotion technologies. A weatherized Nomad was demonstrated in Antarctica in 1999. In this expedition, human assistants placed Nomad's spectrometer on candidate rocks and the rover recorded spectra and classified samples [Apostolopoulos et al, 1999]. With expanded capabilities, Nomad returned to Antarctica in 2000, where it searched for and classified rocks without human assistance. Using a novel autonomous control architecture, specialized science sensing, and Bayesian classification, the Nomad robot classified more than 40 rocks, correctly classifying five as meteorites in Antarctica. Due to strict rules regarding the handling of meteorites, Nomad was limited to evaluating samples in situ and recording their exact location for later recovery by human geologists [Apostolopoulos et al, 2000].

The Sensor arm was developed to provide precise placement of science sensors. The combination of spectral data with visual information has been shown to differentiate meteorites from terrestrial rocks [Pedersen et al, 1998]. However, the acquisition of spectral data is a costly operation in terms of time and complexity. To autonomously perform meteorite classification, Nomad requires the ability to place a pencil sized spectrometer within 1 cm of a potential meteorite.

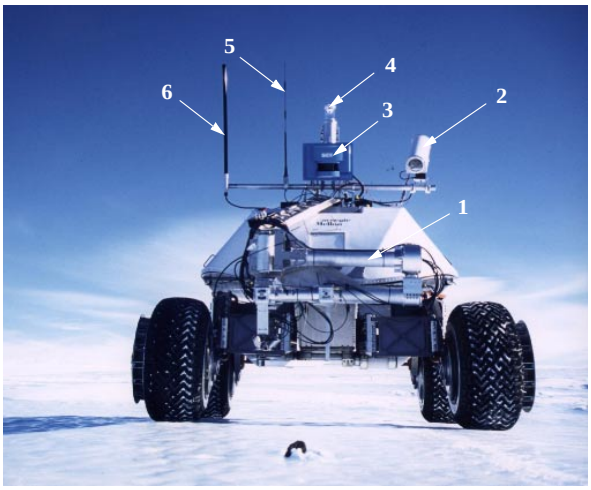

Figure 1: Nomad components: (1)sensor arm (shown stowed), (2) high-resolution science camera, (3) laser range finder, (4) panoramic camera, (5) radio modem antenna, (6) high-gain wireless ethernet antenna.

2. METEORITE SEARCH

Nomad utilizes advanced perception, planning and navigation control to autonomously explore a region. Nomad relies on spectral and visual sensors to detect and classify meteorites. A search is begun when an operator issues a command to search a region designated by differential GPS (DGPS) coordinates. While performing a

search pattern, Nomad autonomously monitors imagery from its high-resolution camera to find dark rocks on the blue-white snow and ice.

A rock sample is selected for investigation considering deployment cost parameters such as distance. Once a sample is selected, Nomad maneuvers so that the sample is in the workspace of the sensor arm (a roughly semi-circular region extending approximately 1.5 meters in front of Nomad). After maneuvers are complete, the high-resolution camera re-acquires an image of the rock and the sensor arm is deployed to the sample. Once the spectrometer is within 1 cm of the sample a visible reflectance spectrum is acquired for identification of the rock sample.

A Bayes-network classifier computes the posterior probability of the rock type being examined, using both imagery and spectral data. Image features used include color and size. A fixed set of spectral features are also used for classification. The classifier differentiates between general types of rocks, such as sedimentary, metamorphic, igneous, extraterrestrial or "other," (generally meaning ice or snow) as well as between specific mineral types such as limestone, granite or stony iron meteorite [Pedersen et al. 2001].

Should the target be given a high probability of being a meteorite, Nomad waits for human validation. If there is another target within the manipulator's workspace, the robot stays in its location and repeats the sensor deployment and classification cycle. Otherwise, Nomad maneuvers to the location of the next target it has identified as a potential meteorite or resumes its search pattern to seek new targets. The autonomous search is complete when Nomad covers the designated area and has classified all identified targets.

3. MECHANICAL DESIGN

The purpose of the sensor arm is to accurately deploy a spectrometer to a rock sample. The arm must avoid interfering with Nomad's maneuverability and must not obscure the field of view of Nomad's various imaging (camera) and safety (laser) sensors.

Table 1: Sensor Arm Specifications

Maximum reach	1.5 m
Maximum payload	2.5 kg
Minimum accuracy	0.5 cm

Initially, the intent was to use an off-the-shelf arm. While typically capable of high speed and high precision, most automated manipulators have a large mass to compensate for dynamic effects. While high speeds (resulting in dynamic effects) are important in factory automation tasks, they are less relevant to the placement of science sensors in the field. Off-the-shelf arms are also generally not designed to operate in harsh antarctic conditions (-20 degrees Celsius, blowing snow etc.) where special components and seals are required. The combination of environmental, performance and cost requirements forced the development of a custom arm.

The design process began by selecting the general

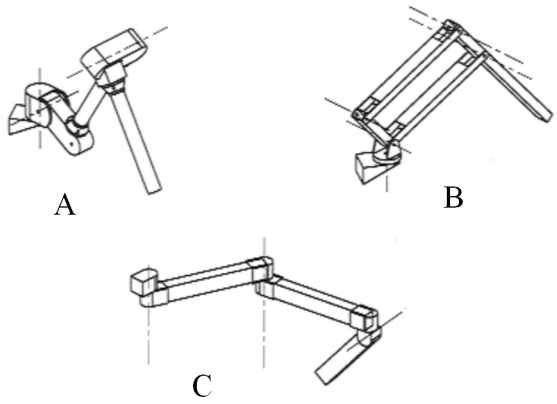

Figure 2: The revolute (A), 5-bar (B) and SCARA concepts (C).

archetype of arm. Under consideration were revolute (elbow), 5-bar linkage, and Selective Compliant Articulated Robot for Assembly (SCARA) concepts.

The revolute manipulator, which includes three rotational joints, can perform a wide range of tasks and is common for factory assembly. Although this type can be extremely dexterous and compact, the torque required at the base joint increase linearly with length of the manipulator.

The 5-bar linkage also contains three rotational joints. However, by using a parallelogram linkage all of the motors can be mounted at the base of the manipulator, removing much of the mass from the arm. Applying constraints to the dynamic equations enables the links to be balanced such that the torque values of joint 1 and joint 2 are independent of joint position, an approach which drastically simplifies the control of the manipulator. The disadvantage is that the linkages require a large swept volume [Spong 1989].

The SCARA manipulator is comprised of two rotational joints and a prismatic joint. The key advantage to this configuration is that gravity does not affect the motion of the first two linkages if the base of the manipulator is level, thus the motors of the first two joints need only compensate for the inertia of the system. Figure 2 shows a SCARA configuration where vertical excursions are accomplished by a rotational joint. A more common configuration uses a linear drive to provide the vertical excursion.

The SCARA configuration was chosen for simplicity of design and control, compactness and minimum joint torque requirements. The decoupling of horizontal and vertical motions simplifies kinematics and software control. The completed arm design uses three identical

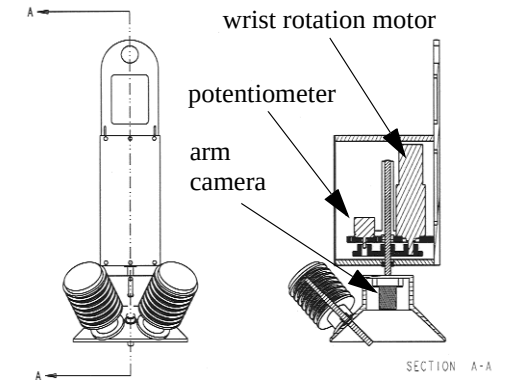

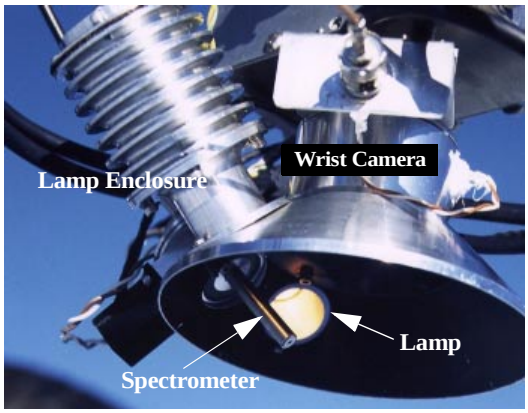

Figure 3: The sensor head.

motors to provide both lateral and vertical motion. The brushless DC (BLDC) motors are coupled to zero backlash harmonic drives which provide high fidelity response to joint commands. Each motor outputs 0.3 Nm of continuous torque which, when passed through a 160:1 reduction, provides an output torque of 48 Nm (before efficiency losses). The motors are sized to allow joint 1 to rotate the fully extended arm with its 2.5 kg sensor payload on a 10 degree slope.

The sensor head (Figure 3) accommodates the spectrometer probe, a downward looking camera (used for visual servoing) and light sources. In addition the sensor head shields the target from direct illumination by the sun. A small brushed motor provides the final wrist rotational degree of freedom.

4. SOFTWARE DESIGN

The overriding principle for software design was design and computational simplicity. Due to limitations placed on processing power, it was not appropriate to perform servoing using high rate video. The desire to minimize the sensor head payload limited sensing to proprioception and a single camera.

4.1 Kinematics

The kinematics of planar, two degree of freedom arms are well understood [Craig, 1989]and can be expressed as:

$$\theta_1 = \text{atan}(y,x) - \text{atan}(k_2,k_1) \quad (1)$$

$$\theta_2 = \text{atan}(s_2,c_2) \quad (2)$$

with:

$$c_2 = \frac{x^2 + y^2 - l_1^2 - l_2^2}{2 l_1 l_2} \quad (3)$$

$$s_2 = \pm\sqrt{1 - c_2^2} \quad (4)$$

$$k_1 = l_1 + l_2 c_2 \quad (5)$$

$$k_2 = l_2 s_2 \quad (6)$$

Target coordinates x and y are defined in a frame of reference centered where the axis of joint 1 intersects the nominal ground plane. The values of θ_1 and θ_2 are bounded to prevent the arm from colliding with Nomad's front wheels. Equation 6 is used to confirm that the commanded position is actually within the arm's work space. If c2 is greater than 1 the target position is unreachable. In this case, Nomad moves, in an attempt to bring the target into the workspace.

Determining the proper joint angle for setting the height of the sensor head is also straightforward, and can be expressed as:

$$\theta_3 = \text{asin}\left(\frac{D-h}{2 l_3}\right) \quad (7)$$

D is the stowed height of the sensor head above flat ground, h is the desired sensor head height and l_3 is the length of each of the descending links.

4.2 Operation

Initial estimates of the target rock's location are transformed into approximate arm coordinates. From this point on, all servoing is performed in arm space, which eliminates the need to precisely determine the transformation between the arm frame and the robot or world frames. This is important since the arm is

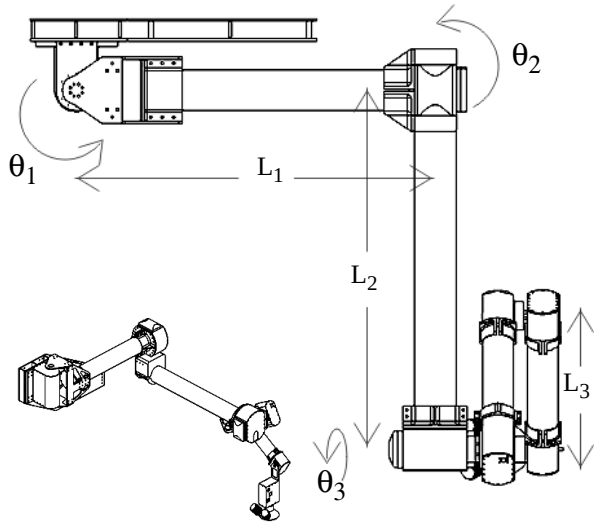

Figure 4: Sensor arm schematics

dismantled for transportation and storage; without this servoing approach, reassembly would lead to changes in the transformation that would require a potentially complicated field recalibration.

In the first step of deployment, the spectrometer is positioned above the estimated position of the rock. Nomad takes an image using the wrist camera and attempts to segment the image into rock and ice/snow. If the segmentation is unable to locate a rock in the image (i.e., the estimated rock position is too poor), a message is sent to the teleoperator who can then remotely adjust the position of the arm so that the servoing procedure can continue. The arm then visually servos to a point 25 cm directly above the actual rock and the sensor head is lowered down onto the rock. The ideal placement of the spectrometer is approximately 5 mm from the surface of the rock at an angle of 45 degrees. This position provides enough reflected light from the rock while minimizing specular reflection. Once in the proper position (Figure 6), the spectrometer samples the rock. After sampling, the sensor head is lifted and the arm is stowed. The entire process typically takes three to four minutes.

4.3 Visual Servoing

The visual servoing task is simplified due to the precision of the mechanical components of the arm. This precision makes a single camera stereo approach viable and straightforward to implement. The steps in the visual servoing algorithm are:

1. Take an initial image from camera position P_1 and locate the centroid of a rock. Estimate its position in arm coordinates (E_1), assuming a flat earth.
2. Servo above the first estimate of the rock, record the camera position P_2 and estimate its position again in arm coordinates (E_2), assuming a flat earth.
3. Generate a line (L_1) between P_1 and E_1 and a second line (L_2) between P_2 and E_2.
4. Find the midpoint of the shortest line segment between L_1 and L_2 and call this the third estimate E_3.
5. Lower the camera to half of its stowed height and generate another pair of estimates and camera positions (P_4 and E_4).
6. Offset by a set amount and then generate another pair (P_5 and E_5).
7. Generate a final position of the rock by repeating steps 3 & 4 with P_4/E_4 and P_5/E_5.
8. Descend to the rock position.

The first two steps of the algorithm move the object from the distorted periphery of the field of view toward the optical center of the camera. Once near the center of the camera, the distortion is minimal and can be ignored.

Lowering the camera and taking the second pair of estimates is an important step for two reasons: the estimates generated at the stowed height are likely erroneous due to camera distortion, and; lowering the camera increases the number of pixels a rock occupies in the image. At the stowed height, each pixel has a projection of about 0.25 x 0.23 cm, which means that a typical 3 cm diameter rock would occupy approximately

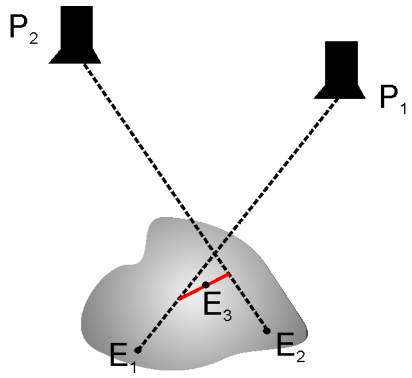

Figure 5: Steps 1 & 2 of the servoing algorithm

120 pixels. Once lowered to 25 cm, the same rock would occupy four times as many pixels, yielding a better centroid and thus a better estimate of the rock position.

Testing highlighted a small position inaccuracy that develops during vertical movement of the wrist. The wrist depends on gravity to remain perpendicular to the ground. Occasionally backlash in the descent mechanism causes a shift in the planar location of the wrist. A final offset step is used to correct for this error.

4.4 Segmentation

One of the biggest problems for both human and robotic meteorite hunters is the broad range of lighting conditions in Antarctica. The conditions change from complete “white outs” where nothing is visible, to clear bright days when shadows and sun glare prevail. For meteorite searches, the best light occurs when there is medium cloud cover which minimizes both shadows and glare.

Figure 6: A typical image from the arm camera.

To segment rocks from background ice, a blue to green color ratio is calculated for each pixel in an image window. Pixels with a low blue-green ratio are designated as rock. Shadowing generally creates several areas of noticeably different blue-green color ratios. The presence of shadows is detected by monitoring the standard deviation of the ratios. A high standard deviation in one of these ratios initiates an intensity-based shadow compensation routine [Shillcutt 2000]. The

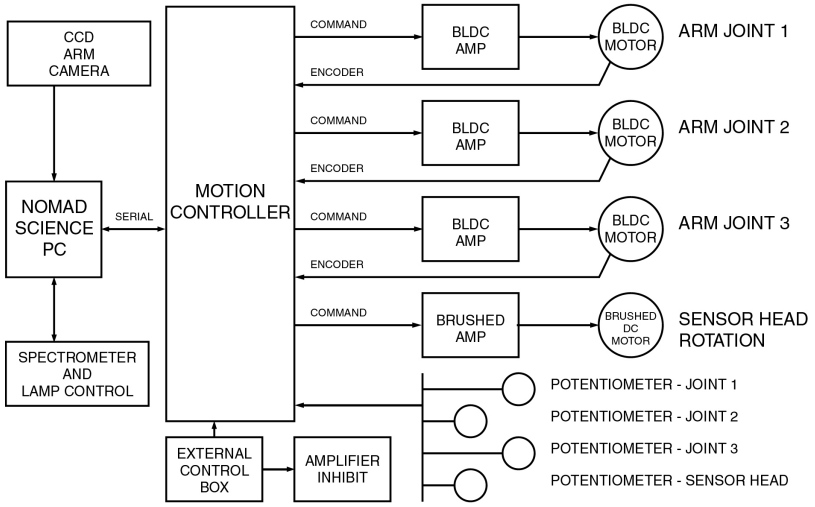

Figure 7: Block diagram of the sensor arm electronics.

circumferences of these regions are found, and the approximate centroids are then calculated. Regions that are too small, too large or too similar to lines (often representative of image artifacts) are ignored.

5. CONTROL ARCHITECTURE

The arm assembly is designed to be a functionally self-contained entity. This was necessary to allow testing while navigation software was undergoing testing and development on Nomad. This approach is reflected in the design of the electrical system. The arm is powered by 24 VDC, which can be supplied by either Nomad or externally. The motion controller, amplifiers and supporting circuitry are housed in an enclosure within Nomad that can be easily removed. The wiring of the arm uses flexible low temperature cabling, sealed connectors and housings to withstand the extreme Antarctic weather conditions.

5.1 Motion Control

To minimize the load on Nomad's computers and to simplify development, a multi-axis motion controller is used to perform low-level control of actuators. Due to the kinematic nature of the task, there is no decrease in performance using an off-the-shelf control solution. By sending simple serial commands, the main control code executing on the science computer can command individual joint positions, velocities and accelerations without having to maintain PID loop control frequencies. This capability also allowed development of the arm software and testing of the arm hardware without interfering with the parallel development and testing of Nomad. The simple interface and command structure of the controller meant that less time had to be devoted to development of the low-level control software.

Position feedback for the arm joints returns to the motion controller from both incremental motor encoders and potentiometers coupled to each of the joints. The potentiometer feedback is used for absolute positioning of the arm while the encoder signals allow for precise relative positioning. Optical limit switches are used to sense the maximum extents of travel.

An external control pendant allows manual control of the prismatic arm actuation and inhibition of the planar joint servos to enable an operator to manually position the arm. The control pendant also provides an emergency stop for all arm motion.

5.2 Instrumentation

A downward looking color CCD camera mounted within the sensor head supplies the system with video input for visual servoing and imaging of the target for identification and archiving.

Spectra of targets are obtained by a reflectance spectrometer consisting of a fiber optic probe mounted on the sensor head and a detector module mounted within Nomad's electronics enclosure. The probe samples the light reflected by the target from two 25 watt quartz halogen lamps each positioned 45 degrees from the probe's optical axis. The lamps provide sufficient incident light so that the effect of scattered sunlight is significantly reduced. The lamps can be extinguished under control of the science computer to allow background compensation of the system. In addition, Nomad can calibrate the spectral response of the sensor head using a standard reflection target mounted just below the spectrometer in the stowed arm position.

6. PERFORMANCE AND RESULTS

In its most recent demonstration, Nomad was sent to Elephant Moraine, Antarctica to conduct autonomous meteorite searches. From January 10-30, 2000 [Apostolopoulos et al, 2000]. Over this time, ten individual demonstrations were performed along with many experiments and data gathering efforts. During the

demonstrations, Nomad deployed the arm to more than 40 samples without failure.

Figure 8: Nomad with the sensor arm deployed.

Empirical measurement confirmed that the arm achieved its goal of sub-centimeter accuracy and achieved millimeter-level precision. The servoing technique proved reliable. Images that were incorrectly segmented, due to unusual lighting conditions, were the primary cause of error for the algorithm. The simplicity and robustness of the servoing approach allowed it to overcome many errors introduced by the segmentation process.

The successful implementation of a high precision ruggedized sensor arm provides a good indication of the state the art in both hardware and software. In terms of hardware the motion controller, motors, harmonic drives, and camera are all off the shelf components that were easily integrated. The arm camera deserves a special note because its small size and weight helped minimize the necessary payload requirement of the arm. The availability of software techniques for the kinematics and visual servoing which are well understood and readily implementable is a major boon. Ten years ago, a fast paced development of this scope would not have been possible.

7. FUTURE WORK

Despite the quality of the servoing and the mechanical accuracy of the arm, the spectral data returned could have been more consistent. Due to the system's inability to characterize the three dimensional shape of investigated rocks, it was impossible to ensure that the spectrometer was angled 45 degrees relative to the surface. This meant that several spectral samples needed to be taken for each rock to acquire at least one good sample.

Current development involves integration of a laser range finder with the sensor head to estimate rock shapes. Using the millimeter-level precision of the arm, the laser will scan the surface of the rock to build a three dimensional model. Surface normals can be extracted from this model and used to determine optimal sensor positioning.

This development will prove to be a first step towards a robotic science capability in extreme environments, and in particular for meteorite search.

8. ACKNOWLEDGMENTS

This program has been supported by the National Aeronautics and Space Administration (NASA) under grants NAG5-7707 and NAG9-1090. The authors would like to thank Melvin Montemerlo, David Lavery and Chris Culbert of NASA for their long-standing support of this work. We would also like to thank the National Science Foundation (NSF) office of polar programs and Antarctic Search for Meteorites (ANSMET) program for providing scientific guidance, field expertise and excellent logistical support.

References

[Apostolopoulos et al, 2000] D. Apostolopoulos, M.D. Wagner, B. Shamah, L. Pedersen, K. Shillcutt, and W.L. Whittaker. Technology and Field Demonstration of Robotic Search for Antarctic Meteorites International Journal of Robotics Research, December, 2000.

[Apostolopoulos et al, 1999] D. Apostolopoulos, M. Wagner, W. Whittaker. Technology and Field Demonstration Results in the Robotic Search for Antarctic Meteorites. Proceedings of the International Conference on Field and Service Robotics, pages 185-190, Pittsburgh, PA, 1999.

[Bapna et al, 1998] D. Bapna et al, The Atacama Desert Trek Outcomes, Proceedings of the 1998 International Conference on Robotics and Automation, Leuven, Belgium, May 1998.

[Craig, 1989] J. Craig. Introduction to Robotics Mechanics and Control. Addison Weasly, Reading, Massachusetts, 1989.

[Pedersen et al, 1998] L. Pedersen, D. Apostolopoulos, W. Whittaker, G. Benedix, T. Roush. Sensing and Data Classification for Robotic Meteorite Search. Proceedings of the 1998 SPIE International Conference on Mobile Robots and Intelligent Transportation Systems, Boston, MA, 1998.

[Pederson et al, 2000] L. Pedersen, M. Wagner, D. Apostolopoulos, W. Whittaker. Autonomous Robotic Meteorite Identification in Antarctica. International Conference in Robotics and Automation, Seoul, Korea, 2001.

[Shillcutt, 2000] K. Shillcutt. Environmental Based Navigational Planning for Robotic Explorers. Ph.D. Thesis, Robotics Institute, Carnegie Mellon University, 2000.

[Spong, 1989] Spong, M.W., M. Vidyasagar, Robot Dynamics and Control, John Wiley & Sons,1989.